Self-similar organization of Gavrilov-Silnikov-Newhouse sinks

Binoy Krishna Goswami*
Laser and Plasma Technology Division, Bhabha Atomic Research Centre, Mumbai 400085, India

Sourish Basu†
Department of Physics, Indian Institute of Technology, Mumbai 400076, India
(Received 9 May 2001; published 13 February 2002)

The numerical analyses of the Hénon map suggest the following features. As we increase the value of the control parameter around each stable period of the period-1 branch, an infinitely large series of period *n*-tupled saddle nodes appears in the following sequence ($n=\ldots,5,4,3$). The limit of each series is the infinitely large set of homoclinic points, created at the homoclinic tangency for the respective flip saddle (boundary saddle in the case of period 1). These observations are in good agreement with the predictions of Gavrilov, Silnikov, and Robinson. Each newly created sink, referred to as Gavrilov-Silnikov (GS) sink, later constitutes a first-order secondary cascade. The flip (boundary) saddles of these cascades also exhibit homoclinic tangency. Past such tangency, around the respective GS sink, an infinitely large series of period *n*-tupled saddle nodes ($n=\ldots,5,4,3$) seems to appear in a similar manner. The newly created GS sinks later constitute second-order secondary cascades. These phenomena, comprised of the homoclinic tangency of a flip (boundary) saddle, followed by the sequential appearance of an infinitely large sequence of period *n*-tupled saddle nodes around the respective GS sink, appear to recur in a self-similar manner, creating higher-order and further higher-order GS sinks and the associated secondary cascades. Each secondary cascade survives within a small subinterval of the control parameter window where the respective GS sink from the immediate lower-order secondary cascade exists. These processes appear to continue *ad infinitum*. Therefore, in the limiting conditions, an infinitely large sequence of sinks may simultaneously coexist in the phase space for an infinitely large number of control parameter values. These observations are in good agreement with the predictions of Newhouse. Thus, the GS sinks may be identified as Gavrilov-Silnikov-Newhouse (GSN) sinks that are organized in a self-similar manner in the phase and parameter space. These features are very similar to those we recently observed in a periodically forced, damped Toda oscillator [B. K. Goswami, Phys. Rev. E **62**, 2068 (2000)]. Since, the Hénon map and Toda oscillator are standard models (one from the maps and the other from the oscillators), our observations may provide some strong evidences towards universality in the self-similar organization of GSN sinks in the low-dissipative limit.

DOI: 10.1103/PhysRevE.65.036210 PACS number(s): 05.45.Ac, 05.45.Pq, 47.52.+j, 42.65.Sf

The two most fascinating fundamental features in nonlinear science are (i) universality and (ii) order (self-similarity) within complexity [1–3]. For instance, let us consider the classic example of chaos that could be an exceedingly complex irregular state of a nonlinear system. Notably, chaos reveals fractal nature in the projected phase space (maps) with inherent self-similarity [4].[1] Such self-similarity has been observed in a large number of nonlinear systems (maps) in the interdisciplinary area of nonlinear science. Thus, the self-similarity is a universal feature of chaos.

From chaos, we draw attention to another complex yet contrasting scenario, predicted by Gavrilov and Silnikov [7], and Newhouse [8]. In the case of one-parameter diffeomorphisms, Gavrilov and Silnikov [7], as we notice from Robinson's theorems *A* and *B* [9], have predicted the sequential appearance of an infinitely large set of sinks [to be referred to as Gavrilov-Silnikov (GS) sinks] in the neighboring parameter space of the homoclinic tangency for a dissipative saddle. Notably, under similar circumstances, Newhouse [8] has predicted (theorem *C* of Robinson [9]) that, in a residual subset in the neighboring parameter space, an infinitely large number of sinks (known as Newhouse sinks) may simultaneously coexist in the phase space. Such a complex scenario has been studied by various researchers to reveal some deeper insight about many intricate issues, namely, the wild hyperbolic sets [9,10], the persistent homoclinic tangency [9–11], zero Lebesgue measure of the set of Newhouse parameter values [12,13], basin boundary metamorphoses [14], basin organizations [15], and some other related phenomena [16,17].

Notably, from the numerical analyses of the periodically forced, damped Toda oscillator model [18] of the class-*B* lasers [19], we have demonstrated [23] the Newhouse sinks in a self-similar bifurcation structure formation [24]. We review here Ref. [23] in brief. Past homoclinic tangency for a period-3 boundary saddle, our observations suggest that, around every stable period (say, of period $3\times2^{m-1}$; $m=1,2,3,\ldots$) of the period-3 branch, an infinitely large sequence of saddle nodes (of period $3n\times2^{m-1}$;

*Email address: bgoswami@apsara.barc.ernet.in
†Email address: n9026014@ccs.iitb.ac.in

[1] In the case of a chaotic state created in the sequence of period doubling, or the union of several such chaotic states via crises [5], the self-similarity of the chaotic orbit may partly be attributed to the fact that the periodic states in Feigenbaum sequence obey a certain scaling phenomenon in the phase space [6].

$n=\ldots,5,4,3$) appears sequentially. The newly created nodes later constitute their period doubling sequences (first-order secondary cascades). Each secondary cascade exists in a subinterval in the control parameter window where the respective sink from the period-3 branch remains stable. Around each stable orbit of these secondary cascades, an infinitely large series of period n-tupled saddle nodes appears sequentially in a similar manner. Each respective node later constitutes a second-order secondary cascade. These phenomena were recurrent in a self-similar manner, creating higher-order and further higher-order secondary cascades, around the period-3 branch. Each secondary cascade exists in a subinterval in the control parameter window where the respective sink (around whom the cascade is created in some process of n tupling) from the immediate lower-order secondary cascade remains stable. Therefore, each stable orbit from any given order secondary cascade coexists in the phase space with the respective stable periodic orbits from all the lower-order secondary cascades. Thus, subject to the choice of parameter values, the limit of such a sequence of coexisting sinks could be infinitely large. In other words, the self-similar appearance of the secondary cascades suggests that an infinitely large sequence of sinks may coexist in the phase space for an infinitely large number of points in the control parameter space, close to the homoclinic tangency of the period-3 boundary saddle. These observations are in good agreement with the predictions of Newhouse. Therefore, these observations suggest in a certain sense some order (self-similarity) within the complex scenario, predicted by Gavrilov, Silnikov, and Newhouse.

In the current paper, we are encouraged to investigate whether the self-similar organization of the Newhouse sinks could be a universal feature. A judicious approach, we believe, would be to investigate the organization of the sinks in another standard model, preferably from maps. We consider the Hénon map that indeed suggests a self-similar organization of the sinks, very similar to what we observed in the Toda oscillator [23].

While presenting the evidence for self-similar organization of the sinks, the current analyses will be more comprehensive, in comparison to our previous work [23], towards a complete identification of the sinks. For example, in the case of the Toda oscillator, we did not investigate the homoclinic tangency of any flip saddle of the period-3 branch. Nor did we do so for any boundary (flip) saddle of any secondary cascade. We believe, such investigations would have helped us to explore the limits of the sequences of the period n-tupled saddle nodes. As a consequence, the possibility that the respective nodes being identified as GS sinks also remained unexplored. In the present paper, we investigate along these directions. Most importantly, our observations will suggest that every homoclinic tangency of the boundary (flip) saddle will be followed with a sequential appearance of infinitely large number GS sinks (created in saddle-node bifurcations). In other words, we will show the self-similar appearance of higher order and further higher order of GS sinks (and the associated secondary cascades). Apparently, each secondary cascade would survive within a small subinterval of the control parameter window where the respective GS sink from the immediate lower-order secondary cascade exists. Therefore, at the limiting conditions, due to self-similarity, one may expect an infinitely large number of coexisting GS sinks at an infinitely large number of parameter values. These observations will be in good agreement with the predictions of Newhouse. Thus, we will identify the GS sinks as Gavrilov-Silnikov-Newhouse (GSN) sinks, organized in a self-similar manner in the phase and parameter space. We consider the Henon map [4,25] described by

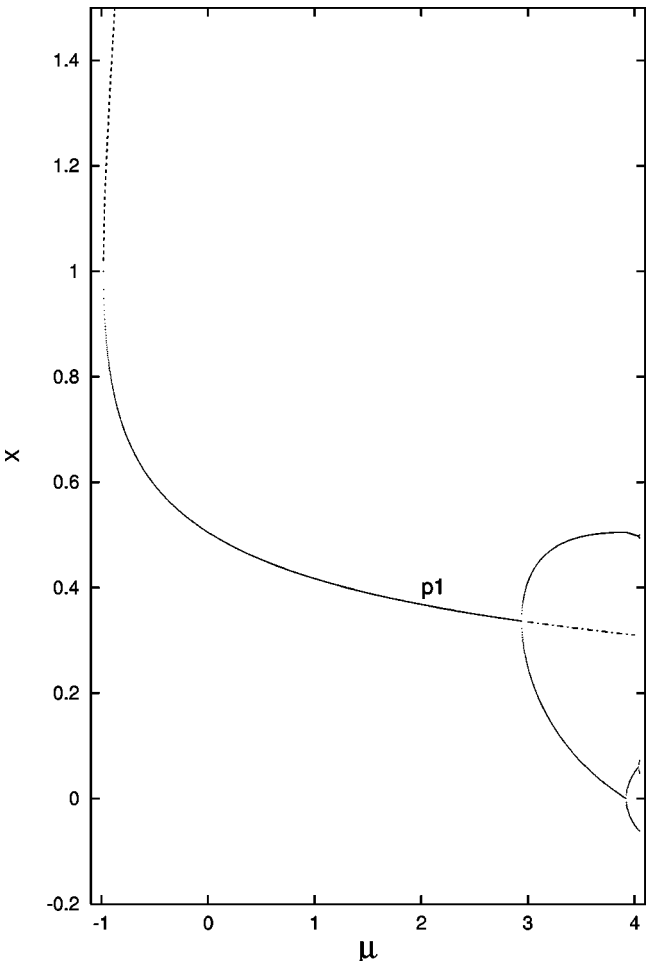

FIG. 1. Bifurcation diagram of the period-1 branch ($p1$). The period-1 boundary and flip saddles are shown by segmented lines.

$$x_{n+1}=1-\mu x_n^2+y_n,$$

$$y_{n+1}=-Jx_n, \tag{1}$$

where $J=0.98$ (a low-dissipative case). In Fig. 1, we show the period 1 branch where the period 1 is created in a saddle-node bifurcation. The invariant manifolds of the period-1 boundary saddle undergo first homoclinic tangency at $\mu=-0.6076$ [Fig. 2(a)]. Past such tangency, as we increase the value of μ further, we observe the sequential occurrence of apparently an infinitely large sequence of period-n($n=\ldots,5,4,3$) saddle nodes around the period-1 sink. The limit of this sequence is the infinite set of homoclinic points, created at the homoclinic tangency. These are in accordance

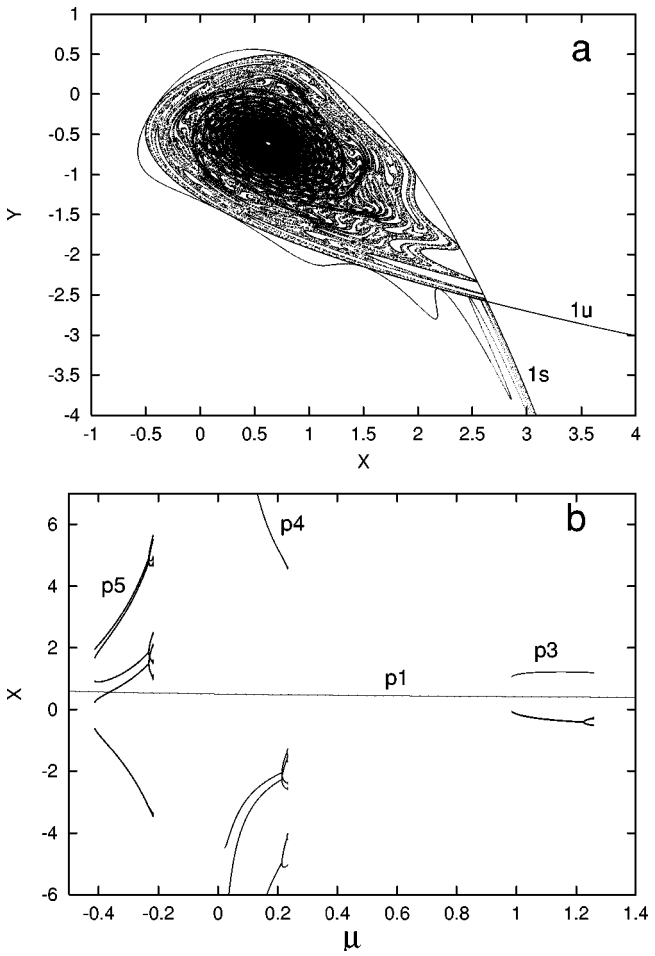

FIG. 2. (a) Homoclinic tangency of the period-1 boundary saddle at $\mu=-0.6076$. The stable and unstable manifolds are, respectively, denoted by $1s$ and $1u$. One component of the stable manifold is accumulating near the other component. Similarly, one component of the unstable manifold is accumulating near the other component. The white spot inside the dense unstable manifold indicates the location of the period-1 sink. (b) The successive appearance of a series of first-order secondary cascades, namely, period-5, -4, and -3 cascades around the period 1. From this figure onwards, a period-n cascade (i.e., a period-n branch) will be denoted by pn.

with the predictions of Gavrilov and Silnikov, thus identifying the nodes as GS sinks. Each sink (say of period-n) later constitutes a first-order secondary cascade (a period-n branch). For instance, in Fig. 2(b), we show the sequential appearance of period-5, -4, and -3 cascades around the period 1. From this figure onwards, a period-n cascade (i.e., a period-n branch) will be denoted by pn. Each cascade exists in a disjoint subinterval of the control parameter window where the period 1 remains stable.[2]

After the period doubling, the period-1 sink becomes a flip saddle and a stable period 2 is created. The invariant manifolds of the period-1 flip saddle also undergo first homoclinic tangency at $\mu=3.222$ [Fig. 3(a)]. Past such tangency, as we increase the value of μ further, again we observe the sequential occurrence of apparently an infinitely large sequence of period-$2n$($n=\ldots,5,4,3$) saddle nodes around the period-2 sink. These observations are in good agreement with Robinson's predictions.[3] The respective GS sinks constitute another series of first-order secondary cascades. For instance, in Fig. 3(b), we show the sequential appearances of period-10, -8, and -6 cascades around the period 2. Each cascade exists in a disjoint subinterval of the control parameter window where the period 2 remains stable. We conjecture that for each successive stage of period doubling in the period-1 branch, one would observe again the homoclinic tangency of the respective flip saddle, followed by sequential appearance of an infinitely large sequence of

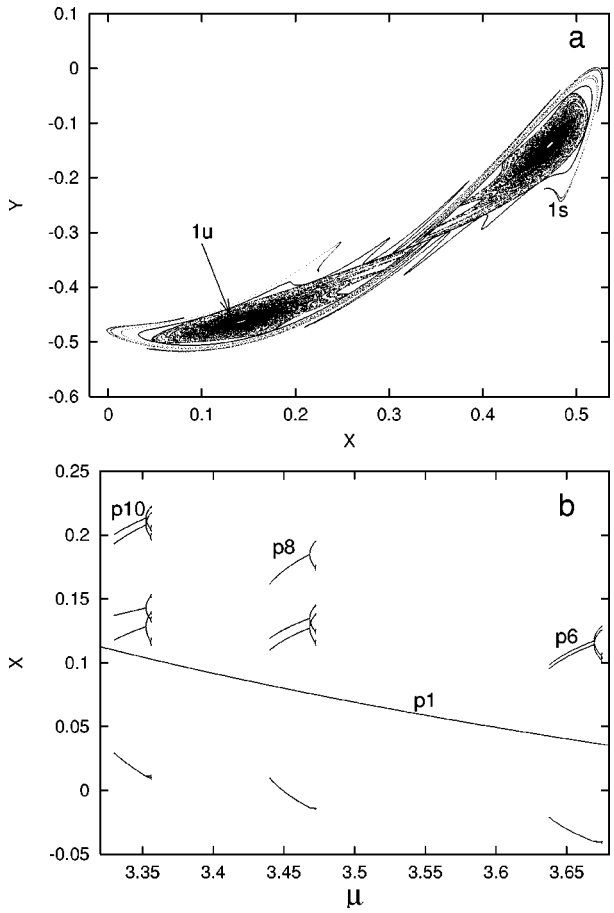

FIG. 3. (a) Homoclinic tangency of the period-1 flip saddle at $\mu=3.222$. The stable and unstable manifolds are, respectively, denoted by $1s$ and $1u$. Two white spots inside the dense unstable manifold indicate the location of period-2 sink. (b) The successive appearance of a series of first-order secondary cascades, namely, period-10, -8, and -6 cascades around period 2. Each cascade and the period-2 sink are sampled every two periods.

[2]Henceforth, by the word ''disjoint'' we imply that each secondary cascade of a given order, created around the same sink, appears in a separate subinterval.

[3]In the case of period doubling, the orientations of the invariant manifolds are not preserved. According to Robinson's theorem *A* [9], the difference of periodicity between successive sinks is twice the periodicity of the flip saddle. This is indeed what we observed.

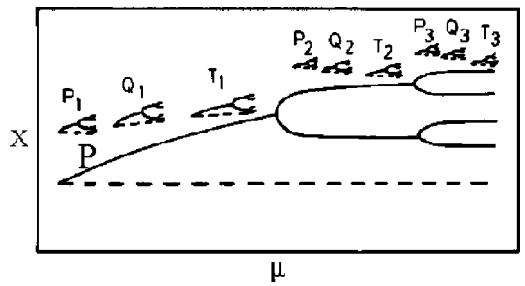

FIG. 4. Schematic illustration of a series of first-order secondary cascades around the sinks of the period-1 branch (denoted by P). The secondary cascades, created around the nth sink (of period 2^{n-1}; $n=1,2,3$) of the period-1 branch, in period tripling, quadrupling, and pentupling are, respectively, denoted by T_n, Q_n, P_n. Only one component of each secondary cascade has been shown. The segmented lines denote the boundary saddles.

period n-tupled first-order GS sinks around the respective sink from the period-1 branch. Each newly created GS sink later will constitute another first-order secondary cascade that will survive within a small disjoint subinterval of the control parameter window where the respective sink from the period-1 branch exists. These features are schematically illustrated in Fig. 4. The period-1 branch is denoted by P. P_n, Q_n, T_n represent the first-order secondary cascades created, respectively, in period pentupling, quadrupling, and tripling around the nth sink of the period-1 branch.

Notably, the boundary saddles of the first-order secondary cascades also undergo homoclinic tangency. Again, each tangency (say of the period-m saddle) is followed by the sequential appearance of an infinitely large sequence of period-mn ($n=\ldots,5,4,3$) saddle nodes around the period-m sink. The limit of such a sequence is the infinitely large set of homoclinic points, created at the respective tangency. These are again in good agreement with the predictions of Gavrilov and Silnikov. The respective GS sinks later constitute a series of second-order secondary cascades. For instance, in Fig. 5(a), we show the homoclinic tangency of the period-3 boundary saddle, and in Fig. 5(b), we show the sequential appearances of period-15, -12, and -9 cascades around period 3. After period doubling ($3\rightarrow 6$), the manifolds of period-3 flip saddle also exhibit homoclinic tangency [Fig. 6(a)]. Past such tangency, an infinitely large sequence of period-$6n$($n=\ldots,5,4,3$) saddle nodes appear around the period-6 sink. The newly created GS sinks later constitute another series of second-order secondary cascades. For instance, in Fig. 6(b), we show the successive appearance of period-30, -24, and -18 cascades around the period 6 of the period-3 branch. In Figs. 7 and 8, we show some more examples that suggest occurrence of similar phenomena around the first two sinks of each of period-4 and period-5 cascades. In Fig. 7(a), we show the successive appearance of period-20, -16, and -12 cascades around the period 4 of the period-4 cascade. In Fig. 7(b), we show the successive appearance of period-40, -32, and -24 cascades around the period 8 of the period-4 cascade. In Fig. 8(a), we show the successive appearance of period-25, -20, and -15 cascades around the period-5 sink. In Fig. 8(b), we show the successive appearance of period-50, -40, and -30 cascades around the period 10 of the period-5

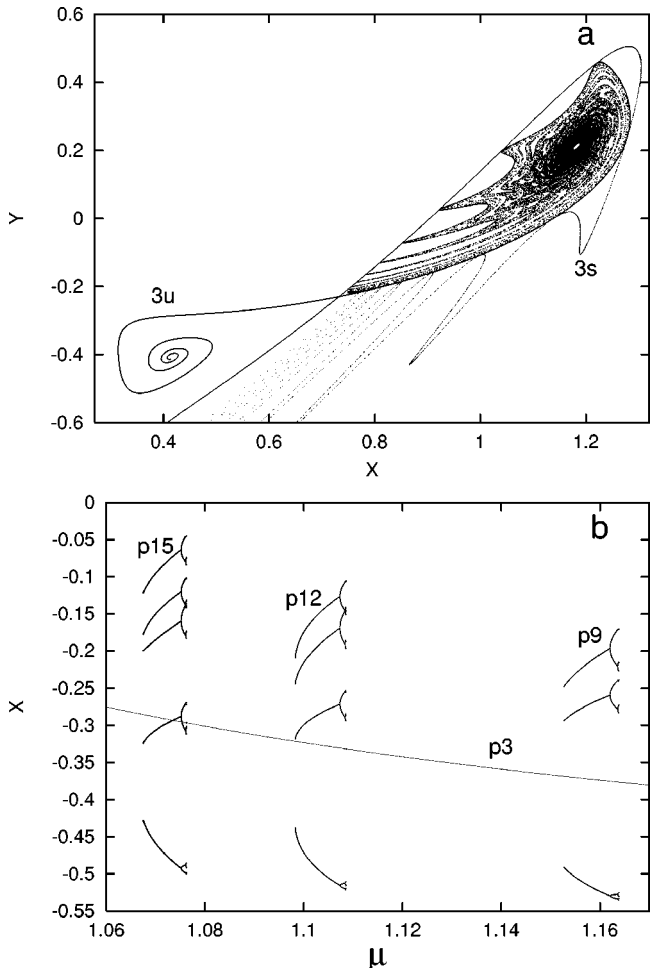

FIG. 5. (a) Homoclinic tangency of the period-3 boundary saddle at $\mu=1.035$. The stable and unstable manifolds are, respectively, denoted by $3s$ and $3u$. The sampling period of the manifolds is three. One component of the unstable manifold (with a few spirals) approaches the period-1 sink. The white spot inside the other dense component indicates the location of the period-3 sink. (b) The successive appearance of a series of second-order secondary cascades, namely, period-15, -12, and -9 cascades around period 3. Each cascade and the period-3 sink are sampled every three periods.

cascade. Each second-order cascade survives within a small disjoint subinterval of the control parameter window where the respective GS sink from the first-order secondary cascade exists. We conjecture that, past the homoclinic tangency of each flip (boundary) saddle of any first-order secondary cascade, one would find an infinite series of second-order GS sinks (and the associated second-order secondary cascades) around the respective first-order GS sink in a similar manner. For a schematic illustration, we may refer back to Fig. 4 where we have to assume the P branch denotes in general any first-order secondary cascade. Also P_n, Q_n, T_n would represent the second-order secondary cascades created, respectively, in period pentupling, quadrupling, and tripling around the nth GS sink of the given first-order secondary cascade P. In Fig. 9, we show some additional evidences of second-order secondary cascades, created around the sinks of period-10, -8, and -6 cascades that are shown earlier in Fig.

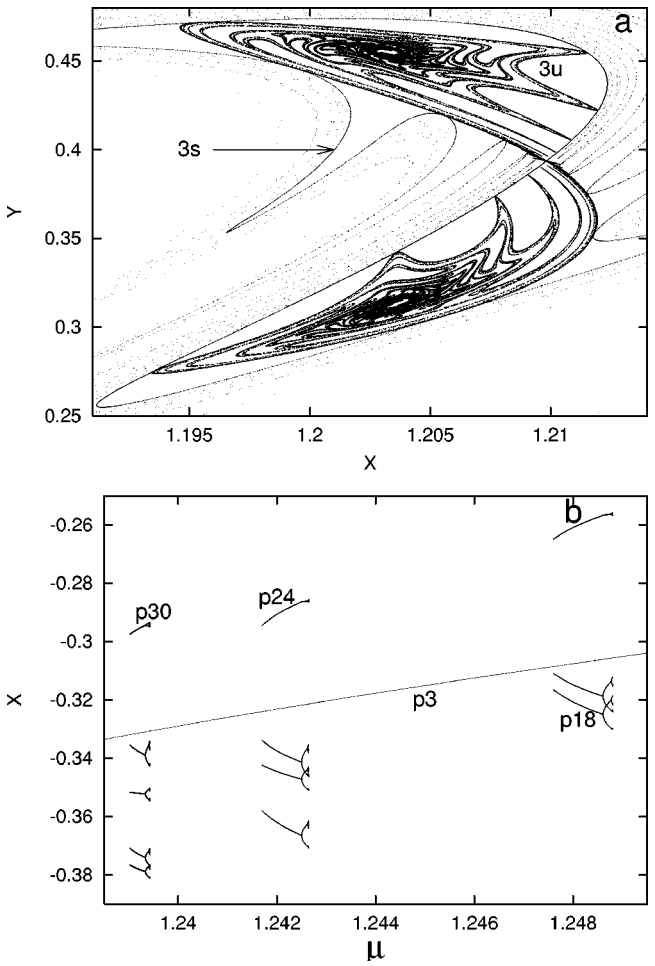

FIG. 6. (a) Homoclinic tangency of the period-3 flip saddle at $\mu = 1.237\,55$. The stable and unstable manifolds are, respectively, denoted by $3s$ and $3u$. The sampling period of the manifolds is three. The white spots inside the core dense regions of the unstable manifold indicate the location of period-6 sink. (b) The successive appearance of a series of second-order secondary cascades, namely, period-30, -24, and -18 cascades around period 6 of the period-3 branch. Each cascade and the period-6 sink are sampled every six periods.

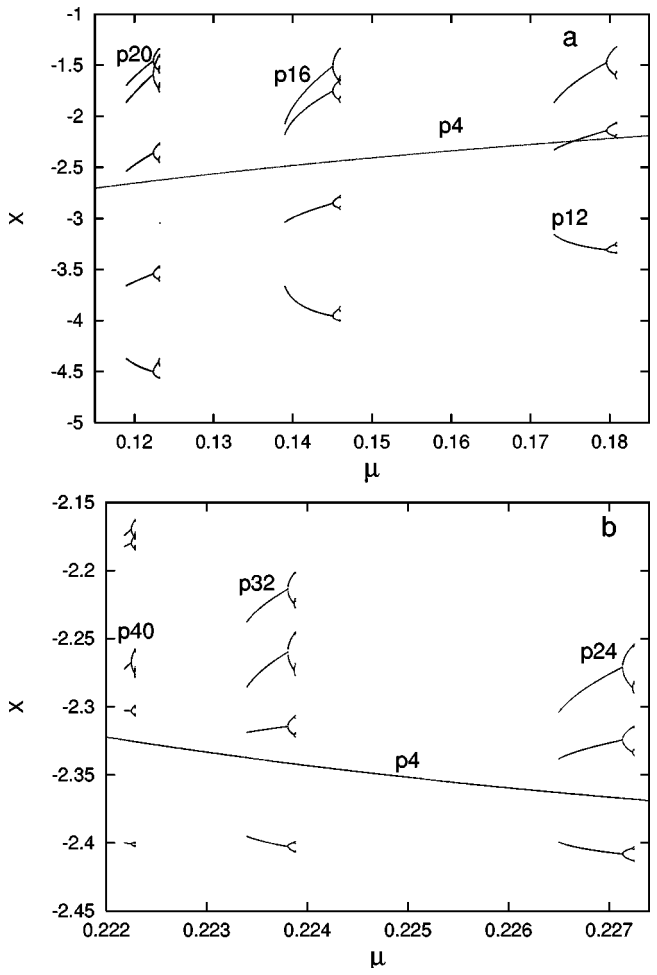

FIG. 7. Successive appearance of some series of second-order secondary cascades around the first two sinks of the period-4 cascade. The period-4 cascade itself is created around period 1 and shown earlier in Fig. 2(b). In each plot, the sampling period is the same as that of the respective sink. (a) Period-20, -16, and -12 cascades around period 4. (b) Period-40, -32, and -24 cascades around period 8.

3(b). In Fig. 9(a), we show the successive appearance of period-30, -24, and -18 cascades around period 6 of period-6 cascade. In Fig. 9(b), we show the successive appearance of period-40, -32, and -24 cascades around the period-8 sink of the period-8 cascade. In Fig. 9(c), we show the successive appearance of period-50, -40, and -30 cascades around the period-10 sink of the period-10 cascade.

Interestingly, the entire phenomena, comprised of the homoclinic tangency of a boundary (flip) saddle, followed by the sequential appearance of an infinitely large sequence of period n-tupled ($n = \ldots,5,4,3$) GS sinks (created in saddle-node bifurcations) around the respective lower-order GS sink seems to recur in a self-similar manner. Also, each newly created GS sink later constitutes a higher-order secondary cascade. For example, we show some third-order secondary cascades in Figs. 10 and 11. In Fig. 10(a), we show the sequential appearances of period-45, -36, and -27 secondary cascades around period 9. Figure 10(b) shows similar appearances of period-60, -48, and -36 cascades around period 12 of period-12 cascade. Figure 11(a) shows sequential appearances of period-75, -60, and -45 cascades around period 15. Finally, in Fig. 11(b), we show an example of the formation of fourth-order secondary cascades around the period-27 sink. We show the sequential appearances of period-135, -108, and -81 cascades around period 27.

These observations suggest a self-similar organization of the GS sinks (and the associated secondary cascades). For schematic illustration, we refer back to Fig. 4 where we assume that P branch represents in general a secondary cascade of any given order. $P_n, Q_n, T_n (n = 1,2,3, \ldots)$ represent the next higher-order secondary cascades created, respectively, in period pentupling, quadrupling, and tripling around nth GS sink of the cascade P. The limit of each GS sequence would be the infinite set of homoclinic points, created at the homoclinic tangency of the respective saddle. Each newly created GS sink starts a new higher-order secondary cascade. Each new cascade survives within a small disjoint subinter-

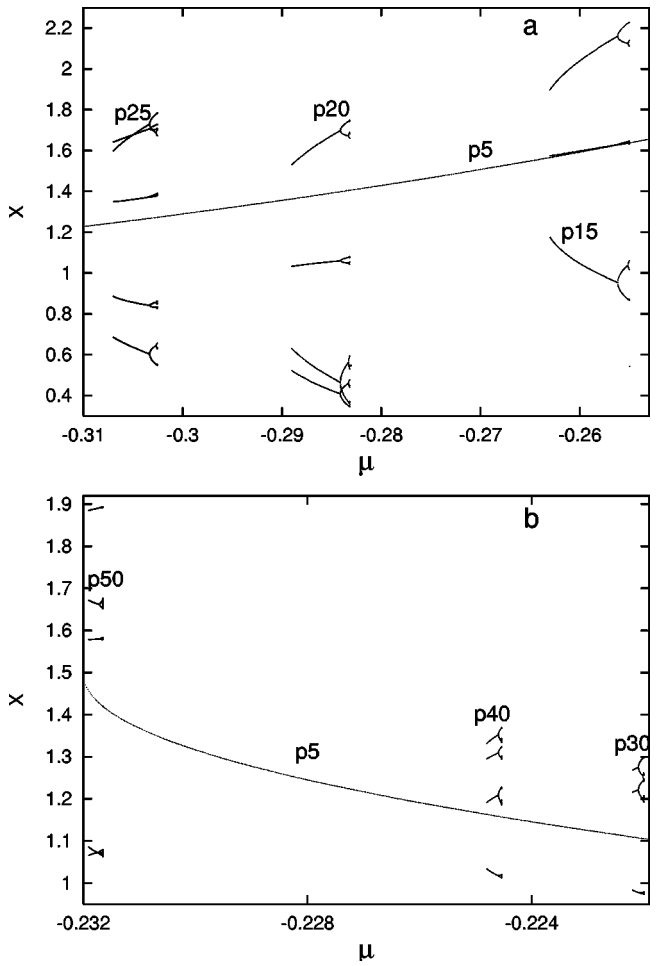

FIG. 8. Successive appearance of some series of second-order secondary cascades around the first two sinks of the period-5 cascade. The period-5 cascade itself is created around period 1 and shown earlier in Fig. 2(b). In each plot, the sampling period is same as that of the respective sink. (a) Period-25, -20, and -15 cascades around period 5. (b) Period-50, -40, and -30 cascades around period 10.

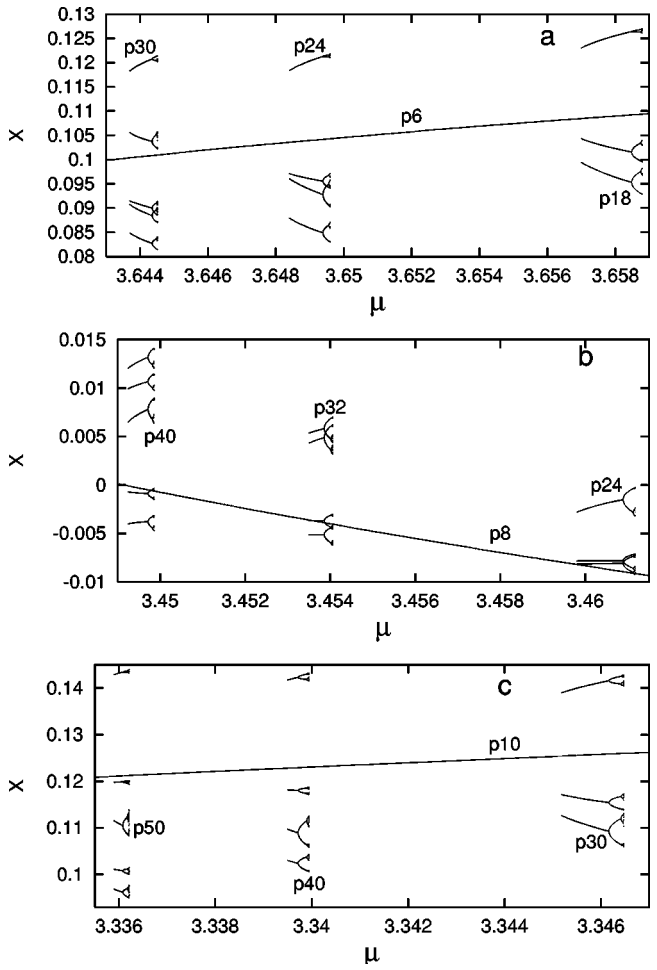

FIG. 9. Successive appearance of some more series of second-order secondary cascades around the sinks of some first-order secondary cascades, created around period 2 [and shown earlier in Fig. 3(b)]. In each plot, the sampling period is the same as that of the respective sink from the first-order cascade. (a) Period-30, -24, and -18 cascades around period 6 of the period-6 cascade. (b) Period-40, -32, and -24 cascades around period 8 of the period-8 cascade. (c) Period-50, -40, and -30 cascades around period 10 of the period-10 cascade.

val of the control parameter window where the respective GS sink from the immediate lower-order secondary cascade exists. Therefore, all the GS sinks from a given order (say nth) secondary cascade coexists in the phase space with the respective GS sinks from all the $(n-1)$ number of lower-order secondary cascade. For instance, in Fig. 12, we show a case where the parameter value is chosen within the window where period 81 remains stable. In this case, we find the coexistence of GS sinks of period-81, -27, -9, and -3 with the period-1 sink. In the phase space, the period 3 is located around period 1, and period 9 around the period 3 [Fig. 12(a)]. Zooming the phase space around period 9, we find period 27 and period 81 around period 27 [Fig. 12(b)].[4] Instead of choosing the parameter value in the period-81 window, if we choose anywhere in the period-108 window, one would observe the period-108 sink in place of the period-81 sink. Similarly, if we choose the parameter value in the window of period 60 [shown earlier in Fig. 10(b)], we shall find the coexistence of GS sinks of periods 3, 12, and 60 with the period-1 sink. Within any of these parameter windows, if one explores further, we believe one may observe further higher-order GS sinks (and the associated higher-order secondary cascades). These phenomena apparently will continue *ad infinitum*. Let us denote the set of control parameter windows for all the first-order secondary cascades (created around the period 1) by S_1. Similarly, let S_2 denote all the control parameter windows for the second-order secondary cascades, which appear around those first-order cascades. It is apparent that $S_2 \subset S_1$. Therefore, $S_1 \cap S_2 = S_2$. Applying the self-similarity, we can similarly state that $S_n \subset S_{n-1}$ where S_n is a similar set for a series of nth-order secondary cascades. Therefore, $S_1 \cap S_2 \cap \ldots \cap S_{n-1} \cap S_n = S_n$. As $n \to \infty$, the

[4]Notice that the distance between the sinks from two consecutive cascades decreases as the order of cascades increases.

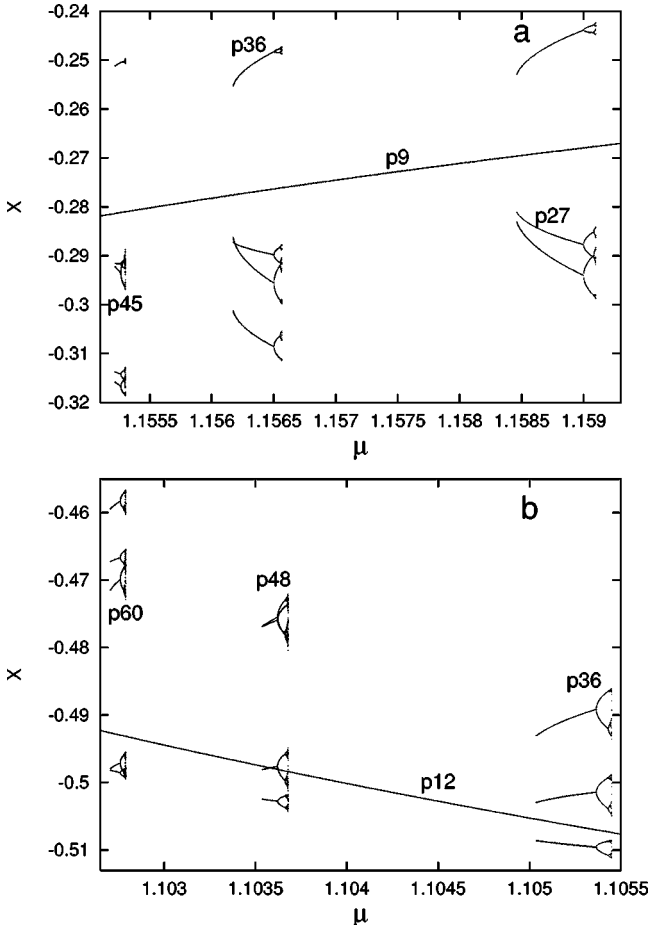

FIG. 10. Successive appearance of some series of third-order secondary cascades around the first sink of each of the period-9 and period-12 cascades. The second-order cascades are shown earlier in Fig. 5(b). In each plot, the sampling period is the same as that of the respective sink. (a) Period-45, -36, and -27 cascades around period 9. (b) Period-60, -48, and -36 cascades around period 12.

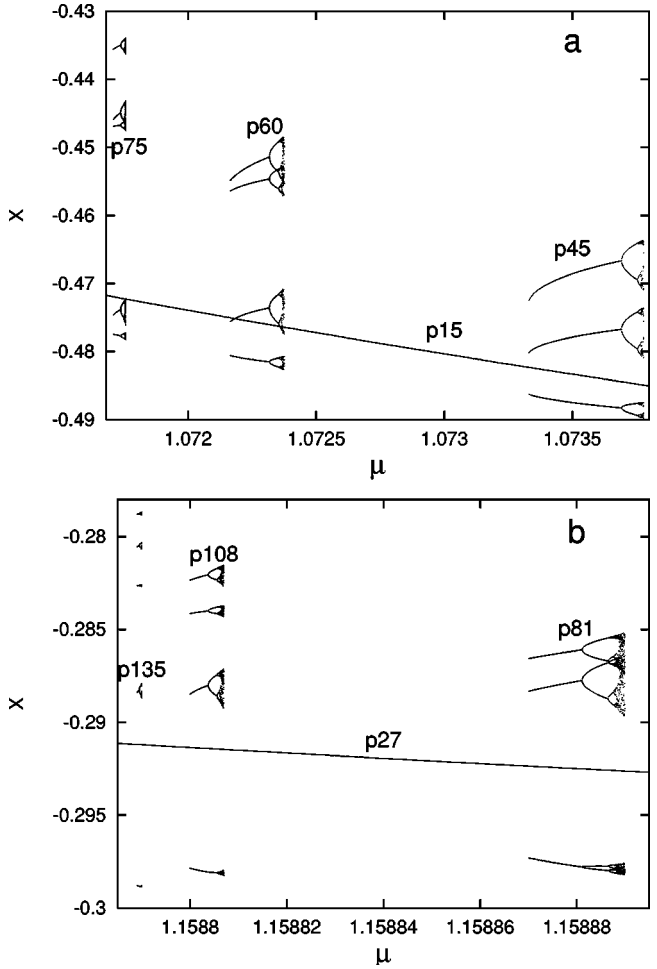

FIG. 11. (a) Successive appearance of some series of third-order secondary cascades around the period-15 sink of the period-15 cascade. The period-15 cascade itself is shown earlier in Fig. 5(b). Period-75, -60, and -45 cascades are found around period 15. The sampling period is 15. (b) The successive appearance of some fourth-order secondary cascades, namely, period-135, -108, and -81 cascades around period 27 of the period-27 cascade. In this plot, the sampling period is 27.

window width of each cascade also tends to zero. Thus, at these limiting conditions, one may find a residual subset (i.e., an infinitely large number of parameter values), where an infinitely large sequence of GS sinks will simultaneously coexist in the phase space. These observations are in good agreement with the predictions of Newhouse, thus identifying the GS sinks as GSN sinks. We may extend a similar argument for the series of secondary cascades that are created around stable period 2, after the homoclinic tangency of the period-1 flip saddle. In this case also, we will reach to the same conclusion. We conjecture that past homoclinic tangency of each flip saddle of the period-1 branch, there will be a residual subset where an infinitely large sequence of GSN sinks will coexist in the phase space. Hence, we demonstrate a self-similar organization of GSN sinks in the low-dissipative limit, created around the period-1 branch in the Hénon map.

In a broad class of one-dimensional, one-parameter maps with one maximum, the order of occurences of stable periodic orbits along the parameter axis follow the *U* sequence [20]. In the case of the Hénon map, which is two parameter and two dimensional, the order of occurence can change as the value of *J* changes [21]. However, the occurrences of stable periodic orbits are not completely independent, as demonstrated by Mindlin *et al.* [22]. They have used a horseshoe implication diagram to construct a minimal set of periodic orbits, which force the existence of all the remaining periodic states associated with a strange attractor, up to any given period. Notably, our analysis suggests that in the low-dissipative limit, a large class of periodic and chaotic orbits is organized in the phase and parameter space in a self-similar manner.

Intuitively, we may find a certain ''genealogy'' in the organization of the orbit structure. For instance, around every node of the period-1 branch, an infinitely large sequence of period-n ($n=\ldots,5,4,3$) saddle nodes appears sequentially. The newly born saddles and nodes may be referred to as ''children,'' while the respective nodes from the period-1 branch may be referred to as ''parents.'' Each child node

later constitutes a first-order secondary cascade. Around each node of this cascade an infinitely large sequence of period-n-tuple ($n=\ldots,5,4,3$) saddle nodes appears in a similar manner. Again, the newly born orbits may be referred to as children of the nodes from the first-order cascades. These phenomena recur in a self-similar manner, giving birth to higher-order and further higher-order ''descendents'' in the genealogical tree. Subject to the values of system parameters, the parent nodes from the period-1 branch may coexist in the phase space along with all their descendents. For instance, in Fig. 12(a), we show period 3 around period 1, and period 9 around period 3. In Fig. 12(b), we find period 27 around period 9, and period 81 around period 27.[5]

The self-similarity here is very similar to what we observe in the driven low-dissipative Toda oscillator [23]. Therefore, we expect that the sinks in Toda oscillator may also be referred to as GSN sinks. Notably, a detailed numerical study of the bifurcation structures of a large number of single-well anharmonic oscillators (which include Duffing, Toda, Morse, and Bubble oscillators) had suggested some qualitative similarity (universality) in the development of the bifurcation structures of these oscillators [26].[6] We expect that the features observed in Toda oscillator may be generic for this class of single-well anharmonic oscillators. Since Henon map is a standard model, in particular, among the maps, we expect that the self-similar organization of the GSN sinks observed in these two standard models, may offer some strong evidence towards establishing universality. Some deeper investigations in other nonlinear systems may confirm our suggestions further.

To conclude, the numerical analyses of a low-dissipative Henon map suggest the following features. As we increase the value of the control parameter, around each stable period of the period-1 branch, an infinitely large series of period n-tupled sinks (created in saddle-node bifurcations) appears in the following sequence ($n=\ldots,5,4,3$). The limit of each series is the infinitely large set of homoclinic points, created at the homoclinic tangency of the respective flip saddle (boundary saddle in the case of period 1). These observations are in good agreement with the predictions of Gavrilov, Silnikov, and Robinson. Thus, we may identify these sinks as Gavrilov-Silnikov sinks. Each GS sink later constitutes a first-order secondary cascade i.e., a branch that survives within a small disjoint subinterval of the control parameter window where the respective sink from the period-1 branch exists. The boundary(flip) saddles of these first-order secondary cascades also exhibit homoclinic tangency. Past such tangency, around the respective GS sink, an infinitely large series of second-order GS sinks seems to appear in a similar manner. The limit of such a series is the infinitely large set of homoclinic points, created at the homoclinic tangency of the respective flip(boundary) saddle from the first-order secondary cascade. Each second-order GS sink later constitutes a second-order secondary cascade that survives within a small subinterval of the control parameter window, where the respective GS sink from the first-order secondary cascade exists. These phenomena, comprising the homoclinic tangency of a flip (boundary) saddle, followed by the sequential appearance of an infinitely large series of period n-tupled GS sinks around the respective lower-order GS sink, appear to recur in a self-similar manner, creating higher-order and further higher-order GS sinks and the associated secondary cascades. Each newly created cascade survives within a small subinterval of the control parameter window where the respective GS sink from the immediate lower-order secondary cascade exists. These phenomena appear to continue *ad infinitum*. Therefore, in the limiting conditions, an infinitely large sequence of GS sinks may coexist in the

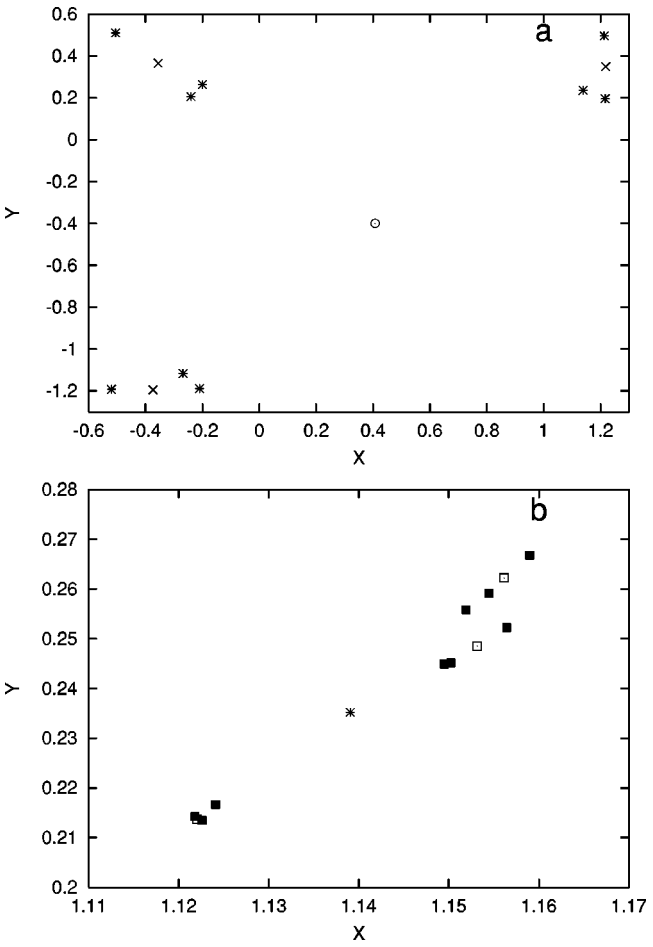

FIG. 12. Simultaneous coexistence of a hierarchy of GS sinks in the phase space; $\mu=1.158\,875$. (a) The period-3 sink (cross signs) around period 1 (circle), and the period-9 sink (star symbols) around the period-3 sink. (b) The period-27 sink (hollow square symbols) around the period-9 sink (star symbol), and the period-81 sink (filled square symbols) around the period-27 sink. In this plot, the sampling period is nine.

[5]The symbolic sequence of coexisting periodic orbits is arranged in a lexicographical manner. If we denote the symbolic sequence of the fundamental (lowest) period by Φ, then the child orbit, born in n tupling, will be described by the symbolic sequence $\Phi\Phi\ldots n$ times. Thus, the lexicographical order of the symbolic sequences of coexisting orbits can be noted.

[6]A detailed list of references, relevant in this context, may also be found in Ref. [27].

phase space for an infinitely large number of control parameter values. These observations are in good agreement with the predictions of Newhouse. So the GS sinks may as well be referred to as Gavrilov-Silnikov-Newhouse sinks. Thus, we demonstrate a self-similar organization of GSN sinks in the phase and parameter space. These features are very similar to those we recently observed in a periodically forced, damped Toda oscillator [23]. Since, the Hénon map and Toda oscillator are standard models (one from maps and the other from oscillators), our observations may provide some strong evidence towards universality in the self-similar organization of GSN sinks in the low-dissipative limit.

We are grateful to Dr. N. Venkatramani, L&PT Division, BARC for his encouragement of our work.

[1] Hao Bai-Lin, *Chaos* (World Scientific, Singapore 1984); P. Cvitanović, *Universality in Chaos* (Adam Hilger Ltd., Bristol, 1984).
[2] F.C. Moon, *Chaotic Vibrations An Introduction for Applied Scientists and Engineers* (Wiley, New York, 1987).
[3] B.B. Mandelbrot, *The Fractal Geometry of Nature* (W. H. Freeman, New York, 1983).
[4] M. Hénon, Commun. Math. Phys. **50**, 69 (1976).
[5] C. Grebogi, E. Ott, and J.A. Yorke, Physica D **7**, 181 (1983).
[6] M.J. Feigenbaum, J. Stat. Phys. **19**, 25 (1978).
[7] N.K. Gavrilov and L.P. Silnikov, Math. USSR Sb. **17**, 467 (1972); **19**, 139 (1973).
[8] S.E. Newhouse, Topology **12**, 9 (1974); Publ. Math. **50**, 101 (1979); *Lectures on Dynamical Systems*, Progress in Math Vol. 8 (Birkhaüser, Boston, 1980).
[9] C. Robinson, Commun. Math. Phys. **90**, 433 (1983).
[10] John Guckenheimer and Philip Holmes, *Nonlinear Oscillations, Dynamical Systems, and Bifurcation of Vector Fields* (Springer-Verlag, New York, 1983); *Elements of Differentiable Dynamics and Bifurcation Theory*, edited by David Ruelle (Academic Press, New York, 1989), Pt. 2.
[11] I. Kan, H. Kocak, and J.A. Yorke, Physica D **83**, 313 (1995).
[12] Laura Tedeschini-Lalli and James A. Yorke, Commun. Math. Phys. **106**, 635 (1986).
[13] Helena E. Nusse and Laura Tedeschini-Lalli, Commun. Math. Phys. **144**, 429 (1992).
[14] C. Grebogi, E. Ott, and J.A. Yorke, Physica D **24**, 243 (1987).
[15] E. Eschenazi, H.G. Solari, and R. Gilmore, Phys. Rev. A **39**, 2609 (1989).
[16] Y-C Lai, C. Grebogi, J.A. Yorke, and I. Kan, Nonlinearity **6**, 779 (1993).
[17] U. Feudel, C. Grebogi, B.R. Hunt, and J.A. Yorke, Phys. Rev. E **54**, 71 (1996).
[18] G.L. Oppo and A. Politi, Z. Phys. B: Condens. Matter **59**, 111 (1985); B.K. Goswami, Phys. Lett. A **190**, 279 (1994); Opt. Commun. **122**, 189 (1996).
[19] F.T. Arecchi, R. Meucci, G. Puccioni, and J.R. Tredicce, Phys. Rev. Lett. **49**, 1217 (1982); B.K. Goswami and D.J. Biswas, Phys. Rev. A **36**, 975 (1987).
[20] N. Metropolis, M.L. Stein, and P.R. Stein, J. Comb. Theory, Ser. A **15**, 25 (1973).
[21] P. Holmes and D. Whitley, Philos. Trans. R. Soc. London, Ser. A **311**, 43 (1984).
[22] G.B. Mindlin, R. López-Ruiz, H.G. Solari, and R. Gilmore, Phys. Rev. E **48**, 4297 (1993).
[23] B.K. Goswami, Phys. Rev. E **62**, 2068 (2000).
[24] B.K. Goswami, Int. J. Bifurcation Chaos Appl. Sci. Eng. **5**, 303 (1995); **12**, 2691 (1997); Phys. Lett. A **245**, 97 (1998).
[25] A.N. Pisarchik and B.K. Goswami, Phys. Rev. Lett. **84**, 1423 (2000).
[26] C. Scheffczyk, U. Parlitz, T. Kurz, W. Knop, and W. Lauterborn, Phys. Rev. A **43**, 6495 (1991).
[27] R. Gilmore and J.W.L. McCallum, Phys. Rev. E **51**, 935 (1995).